Block renormalization study on the nonequilibrium chiral Ising model

Mina Kim (김민아),[1] Su-Chan Park (박수찬),[2] and Jae Dong Noh (노재동)[1,3]
[1]*Department of Physics, University of Seoul, Seoul 130-743, Korea*
[2]*Department of Physics, The Catholic University of Korea, Bucheon 420-743, Korea*
[3]*School of Physics, Korea Institute for Advanced Study, Seoul 130-722, Korea*
(Received 16 July 2014; revised manuscript received 10 December 2014; published 16 January 2015)

We present a numerical study on the ordering dynamics of a one-dimensional nonequilibrium Ising spin system with chirality. This system is characterized by a direction-dependent spin update rule. Pairs of $+-$ spins can flip to $++$ or $--$ with probability $(1-u)$ or to $-+$ with probability u while $-+$ pairs are frozen. The system was found to evolve into the ferromagnetic ordered state at any $u<1$ exhibiting the power-law scaling of the characteristic length scale $\xi \sim t^{1/z}$ and the domain-wall density $\rho \sim t^{-\delta}$. The scaling exponents z and δ were found to vary continuously with the parameter u. To establish the anomalous power-law scaling firmly, we perform the block renormalization analysis proposed by Basu and Hinrichsen [U. Basu and H. Hinrichsen, J. Stat. Mech.: Theor. Exp. (2011) P11023]. The block renormalization method predicts, under the assumption of dynamic scale invariance, a scaling relation that can be used to estimate the scaling exponent numerically. We find the condition under which the scaling relation is justified. We then apply the method to our model and obtain the critical exponent $z\delta$ at several values of u. The numerical result is in perfect agreement with that of the previous study. This study serves as additional evidence for the claim that the nonequilibrium chiral Ising model displays power-law scaling behavior with continuously varying exponents.

DOI: 10.1103/PhysRevE.91.012132 PACS number(s): 02.50.Ey, 05.50.+q, 05.70.Ln

I. INTRODUCTION

Macroscopic systems display an intriguing dynamic scaling behavior upon ordering [1,2]. When a system in an ordered phase is quenched from a disordered configuration, the characteristic size ξ of ordered domains increases with time, and microscopic details become less and less important. Consequently, there emerges a dynamic scaling behavior that is classified into a universality class depending on symmetry, conservation, and so on.

Each universality class is characterized by the power-law scaling of the length scale $\xi \sim t^{1/z}$ with a universal dynamic exponent z. For example, equilibrium systems with a scalar order parameter, such as the Ising model, have $z=2$ under the nonconserved dynamics and $z=3$ under the conserved dynamics in the ordered phase [3,4]. Systems with a vector order parameter also have distinct values of z depending on the presence of the conservation law [3,4].

Recently, the ordering dynamics in a nonequilibrium chiral Ising model (NCIM) was studied numerically in one dimension [5]. The NCIM, which will be explained in detail in Sec. II, has two important features. It has ferromagnetic states with all spins up or down as the two equivalent absorbing states. That is, once the system reaches one of the two ferromagnetic states, it stays there forever. In addition, the NCIM has a direction-dependent spin update rule, which makes the system chiral.

The model without chirality is equivalent to the nonequilibrium kinetic Ising model, whose ordering dynamics is described by $z=2$ [6,7]. When the chirality turns on, the dynamic exponent and the other exponents are found to vary continuously as a function of a model parameter [5]. Such a phenomenon is very rare with only a few examples [8,9]. It might be attributed to the different symmetry property of the NCIM. However, its origin has not been revealed yet.

Basu and Hinrichsen proposed a numerical method to identify a dynamic universality class by using a block transformation [10]. Adopting the idea of the real-space renormalization group transformation [11,12], one divides a one-dimensional lattice of L sites into L/b blocks of size b and coarse-grain configurations. Then, one can measure several correlation functions at the coarse-grained levels. The ratios between the correlation functions turn out to converge to universal values in the $t\to\infty$ limit followed by the $b\to\infty$ limit. This universal feature was tested for some dynamic universality classes [10].

We apply the block renormalization scheme to the NCIM in order to confirm that the NCIM is characterized by the continuously varying critical exponents. In Sec. II, we introduce the NCIM and give a brief review of the numerical result in Ref. [5]. Section III presents results of the block renormalization for the NCIM. These results are fully consistent with the previous numerical results, and they strengthen the claim of the continuously varying critical exponents. The ratio between the block correlation functions is related to the critical exponent through a scaling relation. The scaling relation was proposed in Ref. [10] in the context of the scaling ansatz. We present a microscopic theory for the scaling relation in Sec. IV. We summarize this work with discussions in Sec. V.

II. NONEQUILIBRIUM CHIRAL ISING MODEL

To study the coarsening dynamics of a one-dimensional Ising spin chain $\{s_n=\pm | n=1,\ldots,L\}$ with chirality, the authors have suggested the NCIM with the following dynamic rules [5]:

$$+- \xrightarrow{u} -+, \quad -+ \xrightarrow{\bar{u}} +-,$$
$$+- \xrightarrow{v/2} \begin{matrix}++\\--\end{matrix}, \quad -+ \xrightarrow{\bar{v}/2} \begin{matrix}++\\--\end{matrix}, \tag{1}$$

where $u(\bar{u})$ and $v(\bar{v})$ are the transition rates for the spin exchange and the single spin flip dynamics of the local

configuration $+-$ $(-+)$, respectively. We have assumed periodic boundary conditions. The chirality can be incorporated into the model by taking different transition rates for $+-$ and $-+$ domain walls. The NCIM has two equivalent ferromagnetically ordered states with all spins up or down. These states are absorbing in the sense that the system cannot get out of the states by the above dynamic rules.

In addition to its own merit as a minimal model for the chiral dynamics, the NCIM can be applied to a flocking phenomenon of active Brownian particles by regarding the Ising spin states $+$ and $-$ as the directions of motion of particles in one dimension. The flocking model using active spins is found in Ref. [13].

The chirality breaks the spin up-down symmetry of the Ising model. Unlike the magnetic field, which favors one of the spin states, the chirality does not prefer any of the spin states. In fact, the NCIM is symmetric under the simultaneous inversion of spin and space, $s_n \to -s_{L-n+1}$. In higher dimensions, this chirality turned out to be irrelevant for Ising-like spin models with order-disorder transitions [14] (see also Ref. [15] for a generalization to N-vector models, which showed that chirality is relevant for $N \geqslant 2$). However the one-dimensional system with chirality seems to exhibit intriguing scaling behaviors with continuously varying exponents [5].

It is convenient to map the Ising spin system to a reaction diffusion system of two species A and B by introducing a random variable $\sigma_n \in \{A, B, O\}$: A site n is regarded as being occupied by an A particle $[\sigma_n = A]$ if $(s_n s_{n+1}) = (+-)$. It is regarded as being occupied by a B particle $(\sigma_n = B)$ if $(s_n s_{n+1}) = (-+)$. Otherwise, it is regarded as being empty $(\sigma_n = O)$. Within this scheme, all sites are empty in the absorbing states. Due to the correspondence with Ising spin configurations, the two species should be alternating in space and the number of A particles should be the same as that of B particles. Under the symmetry operation $s_n \to -s_{L-n+1}$, a particle configuration is mapped to the mirror image with the particle species being invariant.

The spin dynamic rules are translated as follows. With rate v species A hops to one of its nearest neighbors chosen with equal probability, and with rate u species A branches two A's at both nearest-neighbor sites and it changes to another species $(A \to ABA)$. The dynamics of species B is the same as above with rates given by the barred parameters. Whenever two species happen to occupy the same site by either a hopping or branching event, both particles annihilate immediately $(A + B \to O)$.

Time evolution of the NCIM with $\bar{u} = \bar{v} = 0$ is illustrated in terms of the spin variable $\{s_n\}$ in Fig. 1(a) and in terms of

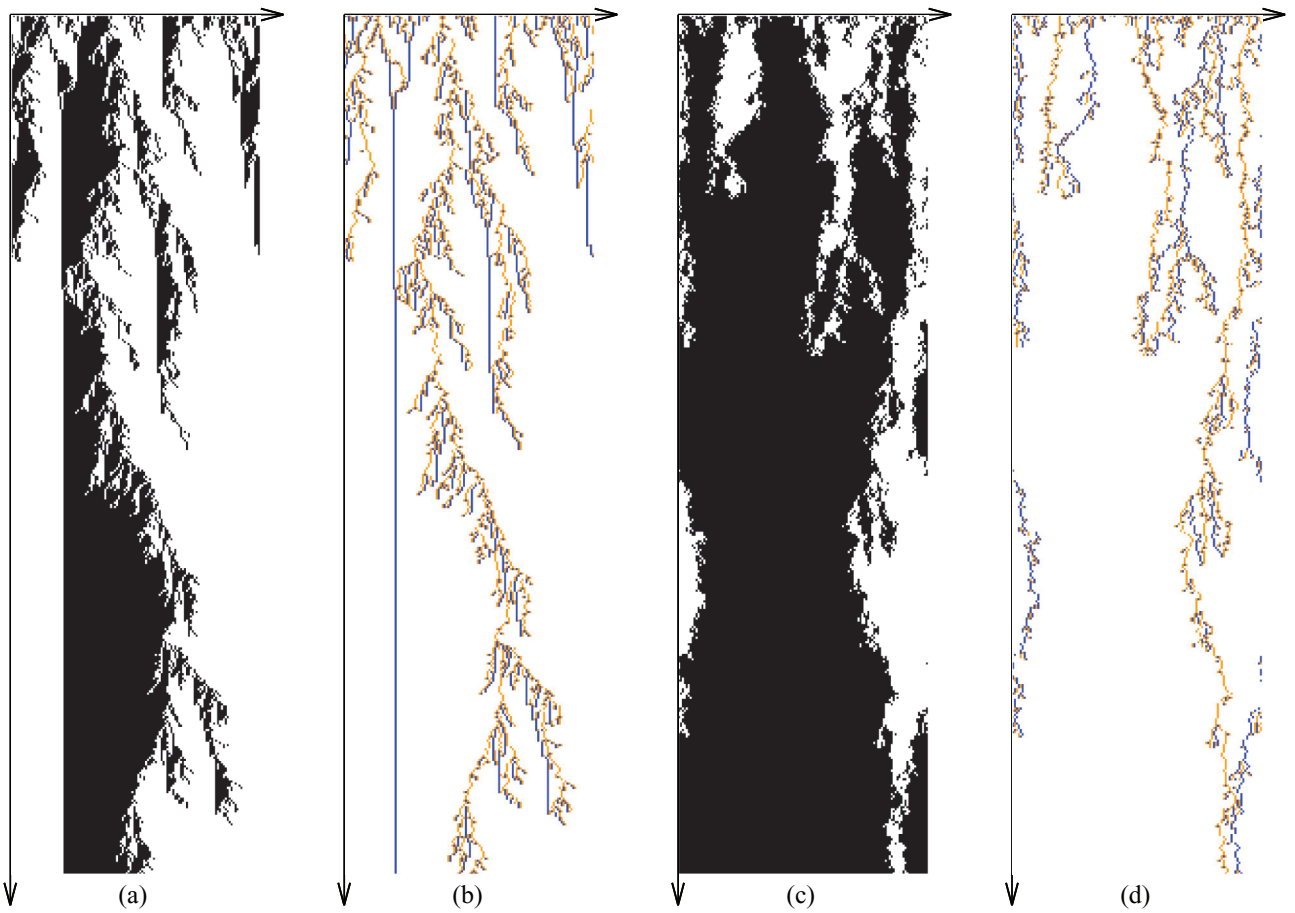

FIG. 1. (Color online) Space-time patterns of the Ising spins with chirality ($\bar{u} = \bar{v} = 0$ and $u = 1 - v = 0.5$) in (a) and (b), and without chirality ($u = v = \bar{u} = \bar{v} = 0.5$) in (c) and (d). Spin dynamics are shown in (a) and (c), where black (white) pixels represent sites of $+$ $(-)$ states. Particle dynamics are shown in (b) and (d), where orange (light) and blue (dark) pixels represent A and B particles, respectively. The horizontal and vertical directions correspond to the spatial and temporal directions, respectively.

the particle variable $\{\sigma_n\}$ in Fig. 1(b). The chirality gives rise to an interesting space-time pattern. The motions of A and B species are asymmetric, while none of the spin states are preferred. As the dynamics proceeds, a characteristic domain size increases and the density of particles decreases with time. The ordering or coarsening dynamics is characterized by the power-law scaling of the characteristic domain size,

$$\xi(t) \sim t^{1/z}, \tag{2}$$

and the domain wall or particle density,

$$\rho(t) \sim t^{-\delta}, \tag{3}$$

with the dynamic exponent z and the density decay exponent δ.

Without chirality [$u = \bar{u}$ and $v = \bar{v}$; see Figs. 1(c) and 1(d)], the NCIM reduces to an exactly solvable model [16] that is equivalent to the branching annihilating walks with two offsprings in Ref. [17]. The exact solution reveals that the ordering dynamics belongs to the universality class of the model at $u = \bar{u} = 0$. It corresponds to the Ising model under the zero-temperature Glauber dynamics [1], or equivalently the voter model [18,19]. The critical exponents are $z = 2$ and $\delta = 1/2$.

When the chirality sets in ($u \neq \bar{u}$ or $v \neq \bar{v}$), the model is not solvable any more. The model has been studied in various regions of parameter space. For example, when $v = \bar{v}$ and $u \neq \bar{u}$, it becomes a mixture of the asymmetric simple exclusion process and the voter model studied in Refs. [20,21]. The ordering dynamics of the NCIM has been studied numerically in Ref. [5]. Surprisingly, the numerical study reveals that the dynamic exponent and the density decay exponent vary continuously within the range $1 < z \leqslant 2$ and $0 < \delta \leqslant 1/2$. We will provide additional evidence for the continuously varying critical exponents in the following sections.

Before delving into the numerical analysis, we would like to add a few remarks. From Fig. 1(b), one may be tempted to associate the continuously varying exponents with the kinetic disorderlike behavior of domain wall B particles and, in turn, with the Griffiths phase [22–24] of systems with quenched disorder. Our observations are not consistent with such a scenario. First, the disorderlike behavior of B particles cannot be regarded as being quenched; it can at best be regarded as an annealed noise in that the position of B domain walls can change by the dynamics of A domain walls. Second, even when B domain walls are allowed to move, the continuously varying exponents have already been observed in Ref. [5]. So it seems hardly likely that the framework of the Griffiths phase can answer the continuously varying exponents behavior.

III. BLOCK RENORMALIZATION ANALYSIS

At criticality, the scaling functions as well as the critical exponents are universal. Extending this idea, Basu and Hinrichsen [10] proposed that the spatial correlation of particle variables in the long-time and large-distance limit can be used in identifying a dynamic universality class. This is accomplished by coarse-graining a microscopic configuration with that of a block variable configuration. As in the real-space renormalization-group transformation [11,12], b sites in a row are coarse-grained by a single block variable. Then, large-distance correlations are measured in terms of the block variables in the $b \to \infty$ limit.

We apply the coarse-graining scheme to the particle or domain-wall variable $\sigma_n \in \{A, B, O\}$ of the NCIM. The coarse-graining should preserve the symmetry and the conservation of the system. It should also preserve the absorbing nature of the vacuum state. The following coarse-graining scheme fulfills the requirements.

To a given block of size b, the number of A and B particles is denoted by $N(A)$ and $N(B)$, respectively. If $N(A) = N(B) = 0$, the block is in a vacuum state and it is assigned to a state O. If $N(A) > N(B)$, the block separates the $+$ domain in the left from the $-$ domain in the right. Thus it is assigned to a state A. If $N(A) < N(B)$, the block separates the $-$ domain in the left from the $+$ domain in the right, so it is assigned to a state B. If $N(A) = N(B) \neq 0$, the block is not in the vacuum state, nor does it separate different domains. Hence we need to assign a block state different from A, B, and O. Furthermore, due to the chirality, we need to assign a different block state depending on whether the domain walls have AB ordering or BA ordering. We will assign a block state X for the former case and Y for the latter. The coarse-graining rule is summarized below:

$$\sigma^b = \begin{cases} O & \text{if} \quad N(A) = N(B) = 0, \\ A & \text{if} \quad N(A) > N(B), \\ B & \text{if} \quad N(A) < N(B), \\ X & \text{if} \quad N(A) = N(B) \neq 0 \text{ and } AB \text{ ordering}, \\ Y & \text{if} \quad N(A) = N(B) \neq 0 \text{ and } BA \text{ ordering}. \end{cases} \tag{4}$$

Note that the block variable σ^b takes on five different states. This is in contrast to the Ising system without chirality, where one needs only three different block states [10]. Due to the chirality, A and B should be distinguished, and so should X and Y. Under the symmetry operation $s_n \to -s_{L-n+1}$, A and B remain the same while X is transformed to Y and vice versa.

For any target configuration $c = (xy\cdots)$, we introduce the correlation function among consecutive block variables,

$$P_c(b,t) = \langle \delta\big(\sigma_n^b(t), x\big)\delta\big(\sigma_{n+1}^b(t), y\big)\cdots \rangle, \tag{5}$$

where $\delta(x,y)$ is the Kronecker delta, $\sigma_n^b(t)$ denotes the block variable at site n at time t, and $\langle\cdot\rangle$ denotes the average over ensembles as well as n. We evaluate numerically the correlation function especially for all two-blocks patterns,

$$\begin{aligned} c \in \{&OO, OA, AO, OB, BO, AB, BA, XO, OX \\ &YO, OY, XA, BX, AY, YB, XX, YY\}. \end{aligned} \tag{6}$$

Patterns AA, BB, XB, AX, BY, YA, XY, and YX are forbidden by the background Ising-spin dynamics. We concentrate on the model with $\bar{u} = \bar{v} = 0$ and $u + v = 1$, which was referred to as the maximum chiral model (MCM) in Ref. [5]. In this model, A particles branch with the probability u and hop with the probability $v = 1 - u$, while B particles are frozen except when the instantaneous pair annihilation ($A + B \to O$) occurs.

Monte Carlo simulations are performed in systems of sizes $L = 2^{24}$ at $u = 0.0$ and 0.1, $L = 2^{23}$ at $u = 0.2$ and 0.3, $L = 2^{22}$ at $u = 0.4$, 0.5, and 0.6, $L = 2^{21}$ at $u = 0.7$, 0.8, and 0.9, and $L = 2^{20}$ at $u = 1.0$. The initial configuration is taken to be the fully occupied state ($\cdots ABAB\cdots$) that is

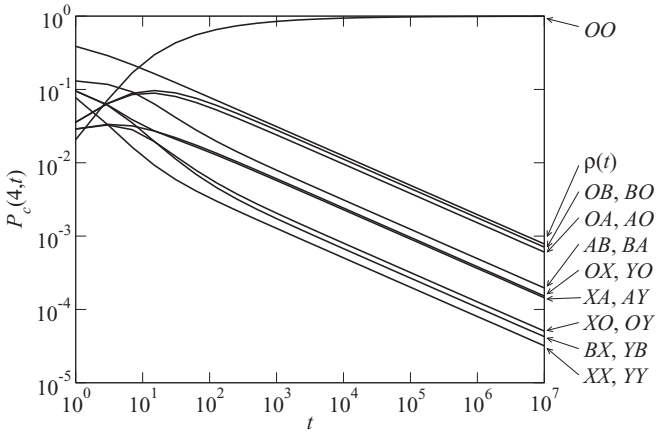

FIG. 2. Temporal decay of the two-block correlation function $P_c(b=4)$ at the model parameter $u=0.3$. Also shown is the overall particle density $\rho(t)$.

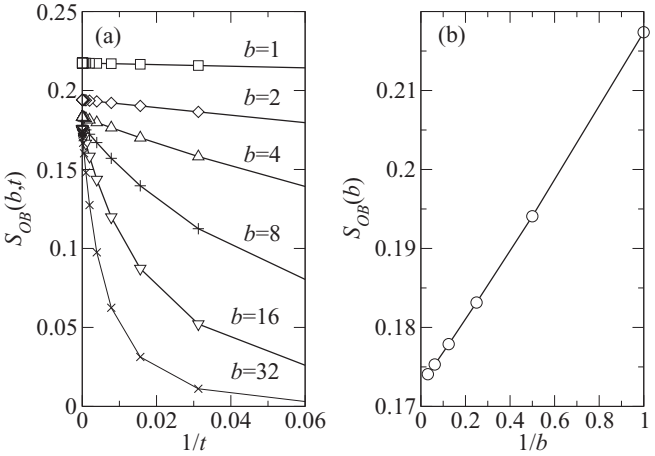

FIG. 3. (a) $S_{OB}(b,t)$ for $b=1,2,\ldots,32$ (from top to bottom) and (b) $S_{OB}(b)$ at the model parameter $u=0.3$.

equivalent to the antiferromagnetic state $(\cdots+-+-\cdots)$. During simulation, the correlation functions $P_c(b,t)$ are evaluated for all two-blocks patterns c in Eq. (6) at times $t=2^l$ with $l\leqslant 24$. The block sizes are $b=2^k$ with $k\leqslant 5$. All the data are obtained by averaging over $N_S\leqslant 5000$ independent samples.

Figure 2 presents the two-block correlation functions with $b=4$ in the MCM with $u=0.3$. After a transient period, all the correlation functions except for the pattern $c=OO$ decay algebraically with the density decay exponent δ. Since the system eventually orders, P_{OO} converges to 1 in the $t\to\infty$ limit. This temporal scaling is also observed for other values of b:

$$P_c(b,t)\sim t^{-\delta}\quad\text{for}\quad c\neq OO. \tag{7}$$

Note that the correlation functions are not independent of each other. The symmetry under $s_n\to -s_{L-n+1}$ requires that

$$\begin{aligned} P_{OA}&=P_{AO},\quad P_{OB}=P_{BO},\\ P_{AB}&=P_{BA},\quad P_{XO}=P_{OY},\\ P_{OX}&=P_{YO},\quad P_{XX}=P_{YY},\\ P_{XA}&=P_{AY},\quad P_{BX}=P_{YB}. \end{aligned} \tag{8}$$

Following Ref. [10], we define

$$S_c(b,t)\equiv\frac{P_c(b,t)}{\sum_{c'\neq OO}P_{c'}(b,t)}=\frac{P_c(b,t)}{1-P_{OO}(b,t)}. \tag{9}$$

It measures the relative frequency of a block pattern c among all patterns but the vacuum pattern OO. Upon taking the ratio, the temporal dependence cancels out and the amplitudes determine $S_c(b,t)$. The scale invariance suggests that the quantity should converge to a universal value [10],

$$S_c=\lim_{b\to\infty}S_c(b) \tag{10}$$

with

$$S_c(b)=\lim_{t\to\infty}S_c(b,t). \tag{11}$$

Figure 3(a) presents the relative frequency $S_{OB}(b,t)$ of a pattern OB at several levels of coarse graining at $u=0.3$. It converges to a constant value $S_{OB}(b)$ in the $t\to\infty$ limit. The extrapolated values are plotted as a function of $1/b$ in Fig. 3(b), from which we can estimate S_{OB}. In practice, we adopted a power-law fitting to the forms $S_c(b,t)=S_c(b)+at^{-\chi}$ and $S_c(b)=S_c+a'b^{-\chi'}$.

Repeating the same procedure, we obtain the relative frequency for all patterns. They are presented in Fig. 4. At $u=0$, A particles diffuse without branching and annihilate in pairs with B particles upon collision. Hence, when $t\gg b^2$, the block configurations consist of isolated A's and B's in the sea of O's. It explains the numerical result that $S_{OB}=S_{BO}=S_{OA}=S_{AO}=1/4$ with the others being zero. At $u=1$, the system reaches an active steady state with a finite particle density. Block variables are equally likely to be in a state of A, B, X, or Y, and a spatial correlation is absent in the $b\to\infty$ limit. Thus, $S_{AB}=S_{BA}=S_{XA}=S_{AY}=S_{BX}=S_{YB}=S_{XX}=S_{YY}=1/8$ and all the others are zero.

As is noticeable in Fig. 4, S_c seems discontinuous at $u=1$. The model at $u=1$ is a singular limit in the sense that there is no chance of falling into absorbing states once the initial particle density is finite. Thus unlike the case of $u<1$, $P_{OO}(b,t)$ cannot approach 1 as $t\to\infty$. We speculate that

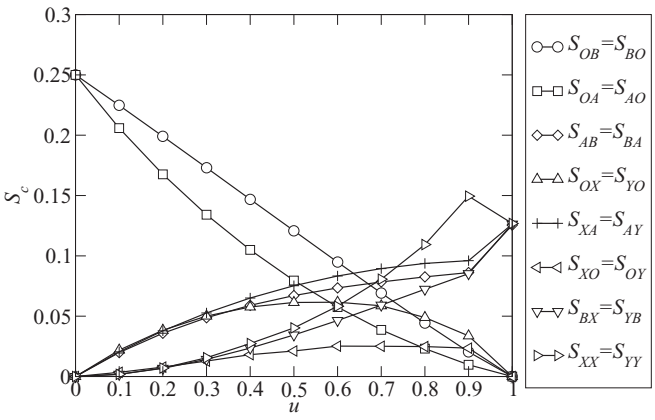

FIG. 4. S_c for two-blocks patterns c. Lines are a guide to the eye.

the sharp change of S_c's near $u = 1$ could be caused because $P_{OO}(b,\infty)$ changes abruptly at $u = 1$.

As the model parameter u varies, each value of S_c varies continuously. Under the hypothesis that S_c should be universal, Fig. 4 provides evidence for the continuously varying critical exponents of the NCIM. In Sec. IV, we will estimate the critical exponent $z\delta$ using the values of S_c's.

IV. CRITICAL EXPONENT $z\delta$

One of the purposes of studying the renormalization group is to estimate the critical exponent. Reference [10] indeed provides a phenomenological theory to connect the block renormalization scheme with the critical exponent $z\delta$ in the large block size limit. In this section, we will discuss the microscopic origin of such a connection and then apply the theory to the NCIM to estimate $z\delta$ from the block transformations.

For general one-dimensional models with absorbing states, one can introduce a random variable ρ_n at each site n ($n = 1,2,\ldots,L$) which takes either 1 or 0. Conventionally, ρ_n is defined in such a way that a configuration is absorbing if and only if $\rho_n = 0$ for all n. In this section, however, we only assume that the condition $\rho_n = 0$ for all n is a necessary condition of systems being in an absorbing state. For example, we may define $\rho_n = 1$ only when a local configuration around n ($s_{n-1}s_ns_{n+1}$) is $(-+-)$ and set $\rho_n = 0$ for any other local configurations. In this example, a configuration with $\rho_n = 0$ for all n is not necessarily absorbing, although an absorbing state should have $\rho_n = 0$ for all n. Still, the average of ρ_n over space and ensemble,

$$\rho(t) = \frac{1}{L}\sum_n \langle \rho_n \rangle, \tag{12}$$

can play the role of an order parameter. The specific choice of ρ_n for actual numerical analyses of the NCIM will be taken later; see above Eq. (44).

For convenience, we will say that a site n is occupied (vacant) if $\rho_n = 1$ (0), even though $\rho_n = 0$ does not necessarily imply that the site n is truly devoid of any particles of the background dynamic model. If we limit ourselves to the stochastic behavior of ρ_n instead of the domain-wall variables σ_n, the block configurations become simpler than those in Sec. III. A block of size b is assigned to be occupied only when it contains at least one occupied site.

Combining Eqs. (2) and (3), the density scales as

$$\rho \sim \xi^{-\alpha} \tag{13}$$

with the exponent

$$\alpha = z\delta. \tag{14}$$

Under the assumption of the scale invariance during the critical dynamics, it is claimed in Ref. [10] that

$$\lim_{b\to\infty}\lim_{t\to\infty}\frac{P_1(b,t)}{P_1(2b,t)} = 2^{-\alpha}, \tag{15}$$

where $P_1(b,t)$ is the probability that a block of size b is occupied, that is, it contains at least one occupied site. Formally speaking, $P_1(b,t)$ is defined as

$$P_1(b,t) = \lim_{L\to\infty}\frac{1}{L}\sum_n \langle 1 - V_{n,b}\rangle, \tag{16}$$

where $V_{n,b} \equiv \prod_{r=0}^{b-1}(1-\rho_{n+r})$ with $V_{n,0} \equiv 1$. Note that $(1 - V_{n,b})$ can be interpreted as the block variable in the sense of Ref. [10]. We will provide a general microscopic theory for the condition under which the relation (15) is valid.

To analyze Eq. (15) systematically, we introduce three types of correlation functions such as

$$P_{\rho\rho}(r,t) = \frac{1}{L}\sum_n \langle \rho_n\rho_{n+r}\rangle, \tag{17}$$

$$P_{\rho v\rho}(r,t) = \frac{1}{L}\sum_n \langle \rho_n V_{n+1,r-1}\rho_{n+r}\rangle, \tag{18}$$

$$P_{v\rho}(r,t) = \frac{1}{L}\sum_n \langle V_{n,r}\rho_{n+r}\rangle. \tag{19}$$

Taking the translational invariance for granted, $P_{\rho\rho}(r,t)$ is the joint probability that two sites separated by a distance r are occupied simultaneously. Similarly, $P_{\rho v\rho}(r,t)$ denotes the joint probability that two sites separated by a distance r are occupied with all intermediate sites being vacant. $P_{v\rho}(r,t)$ is the joint probability that a site is occupied and preceded by r empty sites. For example, $P_{\rho v\rho}(1,t) = \langle \bullet\bullet\rangle$, $P_{v\rho}(1,t) = \langle \circ\bullet\rangle$, $P_{\rho v\rho}(2,t) = \langle \bullet\circ\bullet\rangle$, $P_{v\rho}(2,t) = \langle \circ\circ\bullet\rangle$, and so on, where $\bullet$ ($\circ$) signifies an occupied (a vacant) site.

The first step is to represent $\rho(t)$ and $P_1(b,t)$ in terms of these correlation functions. The identity $V_{n,1} + \rho_n = 1 (\circ + \bullet = 1)$ yields that $\rho(t) = P_{v\rho}(1,t) + P_{\rho v\rho}(1,t) (\langle\bullet\rangle = \langle\circ\bullet\rangle + \langle\bullet\bullet\rangle)$ and $P_{v\rho}(r-1,t) = P_{\rho v\rho}(r,t) + P_{v\rho}(r,t) (\langle\circ\cdots\bullet\rangle = \langle\bullet\circ\cdots\bullet\rangle + \langle\circ\circ\cdots\bullet\rangle)$. Applying the second relation iteratively, we get, for any $1 \leqslant b \leqslant L$,

$$\rho(t) = \sum_{r=1}^{b} P_{\rho v\rho}(r,t) + P_{v\rho}(b,t). \tag{20}$$

In the following discussion, the $L \to \infty$ limit is assumed to be taken first. Note that under the thermodynamic limit, $\rho(t) > 0$ for finite t once $\rho(t=0) > 0$ and no sample can fall into an absorbing state up to finite t.

Using the identity $V_{n,1} = 1 - \rho_n$ again, one can decompose $V_{n,b} = V_{n,b-1}V_{n+b-1,1}$ into $V_{n,b} = V_{n,b-1} - V_{n,b-1}\rho_{n+b-1}$. Hence, we obtain $P_1(b,t) = P_1(b-1,t) + P_{v\rho}(b-1,t)$. Applying the relation iteratively and using $P_1(1,t) = \rho(t)$, we can rewrite $P_1(b,t)$ as

$$\begin{aligned} P_1(b,t) &= \rho(t) + \sum_{r=1}^{b-1} P_{v\rho}(r,t) \\ &= \rho(t) + \sum_{r=1}^{b-1}\left(\rho(t) - \sum_{k=1}^{r} P_{\rho v\rho}(k,t)\right) \\ &= b\rho(t) - \sum_{r=1}^{b}(b-r)P_{\rho v\rho}(r,t), \end{aligned} \tag{21}$$

where the relation (20) is used in the second line. Consequently, we obtain

$$R(b,t) \equiv \frac{P_1(b,t)}{P_1(2b,t)} = \frac{b - \sum_{r=1}^{b}(b-r)F(r,t)}{2b - \sum_{r=1}^{2b}(2b-r)F(r,t)}, \quad (22)$$

where

$$F(r,t) \equiv P_{\rho v\rho}(r,t)/\rho(t). \quad (23)$$

It can be interpreted as the conditional probability of $V_{n+1,r-1}\rho_{n+r} = 1$ given that $\rho_n = 1$. Namely, $F(r,t)$ is the probability that a given particle at time t would find its first-neighbor particle at distance r.

From Eq. (20), we find a normalization condition

$$\sum_{r=1}^{b} F(r,t) + \frac{P_{v\rho}(b,t)}{\rho(t)} = 1. \quad (24)$$

According to the probability interpretation of $F(r,t)$ above, we can claim that

$$\sum_{r=1}^{\infty} F(r,t) \equiv \lim_{b\to\infty} \sum_{r=1}^{b} F(r,t) = 1, \quad (25)$$

which is equivalent to

$$\lim_{b\to\infty} \frac{P_{v\rho}(b,t)}{\rho(t)} = 0 \quad (26)$$

for any t. Since $\rho(t)$ is finite for finite t, Eq. (26) should be satisfied because the mean distance between two occupied sites should be $1/\rho(t)$. Recall that the thermodynamic limit is assumed to be taken already.

It is quite tempting to claim that

$$\lim_{b\to\infty}\lim_{t\to\infty} \frac{P_{v\rho}(b,t)}{\rho(t)} = 0 \quad (27)$$

and

$$\sum_{r=1}^{\infty} F_\infty(r) = 1, \quad (28)$$

where $F_\infty(r) = \lim_{t\to\infty} F(r,t)$. Unfortunately, however, this is not always true. A counter example can be found from the pair annihilation model ($A + A \to 0$). In this example, we define ρ_n such that $\rho_n = 1$ if a particle is present at site n and 0 otherwise. Since $\rho(t) \sim t^{-1/2}$ and $P_{\rho\rho}(r,t) \sim rt^{-3/2}$ [25–28], we get

$$0 \leqslant F(r,t) \leqslant P_{\rho\rho}(r,t)/\rho(t) \sim t^{-1}, \quad (29)$$

where we have used $P_{\rho v\rho}(r,t) \leqslant P_{\rho\rho}(r,t)$. Thus, $F_\infty(r) = 0$ for all r, which cannot be consistent with Eq. (28).

The normalization condition Eq. (28) for $F_\infty(r)$ is not satisfied when vacant sites form an infinite interval in the $t \to \infty$ limit. Therefore, we introduce a parameter $0 \leqslant \phi \leqslant 1$ such that

$$\sum_{r=1}^{\infty} F_\infty(r) = 1 - \phi. \quad (30)$$

Then, the numerator of Eq. (22) can be written as

$$G(b) \equiv b - \sum_{r=1}^{b}(b-r)F_\infty(r)$$

$$= b\phi + b\sum_{r=b+1}^{\infty} F_\infty(r) + \sum_{r=1}^{b} rF_\infty(r). \quad (31)$$

Assuming the scale invariance, we expect $F_\infty(r) \sim r^{-\theta}$ with a critical exponent θ which should be larger than 1 by Eq. (30). Within this assumption, one can easily see that

$$b\sum_{r=b+1}^{\infty} F_\infty(r) \sim \sum_{r=1}^{b} rF_\infty(r) \sim b^{\min[0,2-\theta]} \ll b \quad (32)$$

for large b.

Suppose that ϕ is strictly positive. Then, $G(b) \simeq bc + O(b^{\min[0,2-\theta]})$ and

$$\lim_{t\to\infty} R(b,t) = 2^{-1}, \quad (33)$$

which gives $\alpha = 1$. The pair annihilation model belongs to this category with $\phi = 1$. Since the model is characterized with $z = 2$ and $\delta = 1/2$, the relation (15) appears to be valid. However, we believe that this coincidence is fortuitous. As a counter example, consider the two-species diffusion-limited annihilation model ($A + B \to 0$) and interpret ρ_n as the particle occupation number irrespective of species. If the system evolves from a random initial condition, $\rho(t) \sim t^{-1/2z}$ with $z = 2$ [29–32]. Since interparticle distances diverge as $1/\rho \sim t^{1/2z}$ and there is no branching event that can place a particle close to a given particle, $F_\infty(r)$ should be 0 for finite r. Thus, Eq. (15) leads to $\alpha = 1$, which is different from $z\delta = 1/2$. In other words, unlike the general idea of the renormalization group, Eq. (15) has limited applicability when the normalization in Eq. (28) fails.

If the normalization is valid ($\phi = 0$) and $F_\infty(r) \sim r^{-\theta}$ for large r, the asymptotic behavior of $G(b)$ becomes

$$G(b) \sim \begin{cases} b^{2-\theta}, & 1 < \theta < 2, \\ \ln b, & \theta = 2, \\ \text{const}, & \theta > 2, \end{cases} \quad (34)$$

which results in

$$\lim_{b\to\infty}\lim_{t\to\infty} R(b,t) = \begin{cases} 2^{-(2-\theta)}, & 1 < \theta < 2, \\ 1, & \theta \geqslant 2. \end{cases} \quad (35)$$

Assuming that Eq. (15) is valid with $\alpha = z\delta$ for any θ, Eq. (35) suggests that α should be zero for $\theta \geqslant 2$. Since z cannot be zero, δ should be zero if $\theta \geqslant 2$. That is, the system with $\theta \geqslant 2$ should be in the active phase and $F_\infty(t)$ should actually decay exponentially. Thus, the necessary conditions that a *critical* system satisfies Eq. (15) are Eq. (28) and $F_\infty(r) \sim r^{-\theta}$ with $1 < \theta < 2$ (or $\alpha < 1$) for sufficiently large r.

Assuming that all necessary conditions are satisfied, we will now argue that $2 - \theta$ is indeed equal to α. We start from the observation that

$$\langle \rho_i \rho_{i+r} \rangle = P_{\rho v\rho}(r,t) + \sum_{k=1}^{r-1} \langle \rho_i V_{i+1,k-1} \rho_{i+k} \rho_{i+r} \rangle, \quad (36)$$

where we have exploited the translational invariance of the system. Employing a cluster mean-field-type approximation such that

$$\langle \rho_n V_{i+1,k-1} \rho_{n+k} \rho_{n+r} \rangle \approx \frac{P_{\rho v\rho}(k,t) P_{\rho\rho}(r-k,t)}{\rho(t)}, \quad (37)$$

we get

$$C_\infty(r) \approx F_\infty(r) + \sum_{k=1}^{r-1} F_\infty(k) C_\infty(r-k), \tag{38}$$

where $C_\infty(r) = \lim_{t\to\infty} P_{\rho\rho}(r,t)/\rho(t)$. Introducing generating functions

$$\widetilde{C}_\infty(s) = \sum_{r=1}^{\infty} e^{-sr} C_\infty(r), \quad \widetilde{F}_\infty(s) = \sum_{r=1}^{\infty} e^{-sr} F_\infty(r), \tag{39}$$

and using the convolution theorem, we get

$$\widetilde{C}_\infty(s) \approx \frac{\widetilde{F}_\infty(s)}{1-\widetilde{F}_\infty(s)}. \tag{40}$$

From the scale invariance, we expect $C(r) \sim r^{-\alpha}$ and, in turn,

$$\widetilde{C}_\infty(s) = \sum_{r=1} C_\infty(r) e^{-sr} \approx \int_1^\infty r^{-\alpha} e^{-sr} dr$$
$$\sim s^{-(1-\alpha)} \int_0^\infty u^{-\alpha} e^{-u} du \sim s^{-(1-\alpha)}, \tag{41}$$

which diverges as $s \to 0$ if $\alpha < 1$ (recall that this is one of the necessary conditions). Since $\widetilde{F}_\infty(s) \to 1$ as $s \to 0$ due to Eq. (28), $1-\widetilde{F}_\infty(s)$ should approach 0 as $s \to 0$ for Eq. (40) to be valid. For small s, we obtain

$$1-\widetilde{F}_\infty(s) = \sum_{r=1}^{\infty} F_\infty(r)(1-e^{-sr}) \approx \int_1^\infty r^{-\theta}(1-e^{-sr}) dr$$
$$= s^{\theta-1} \int_s^\infty u^{-\theta}(1-e^{-u}) du. \tag{42}$$

When $1 < \theta < 2$, the integral part converges to a finite constant as $s \to 0$, so $1-\widetilde{F}_\infty(s) \sim s^{\theta-1}$. Plugging this into Eq. (40), we obtain the scaling relation

$$\theta = 2 - \alpha. \tag{43}$$

If we use the scaling relation in Eq. (35), we finally arrive at the relation (15) with $\alpha = z\delta$.

The scaling relation (43) is tested numerically for the NCIM. We measured the correlation functions $F(r,t)$ and $C(r,t)$ numerically in Monte Carlo simulations. Figure 5 presents the numerical data for the system of size $L = 2^{20}$ with the parameters $u = 1-v = 0.3$ and $\bar{u} = \bar{v} = 0$. The correlation functions follow a power law in the regime $r \ll t^{1/z} \ll L$. The power law justifies the requirement for the scaling argument. We also plot the product of $C(r,t)$ and $F(r,t)$. It follows the power law with the exponent -2, which verifies the scaling relation (43). The same results are obtained from other values of u (details not shown here). Thus, we expect that the cluster mean-field approximation leads to the correct scaling relation.

The remaining question is why this cluster mean-field-type approximation should be accurate even though the fluctuation is crucial in one dimension. The cluster mean-field-type approximation has the same spirit as the independent interval approximation [25,33,34], which successfully described the domain size distribution in reaction diffusion systems. Of course, a successful approximation in one model does not necessarily imply applicability to any other models. It would be an interesting theoretical challenge to understand the applicability of the cluster mean-field-type approximation Eq. (37), but this is beyond the scope of this work. We defer this question to later works [35].

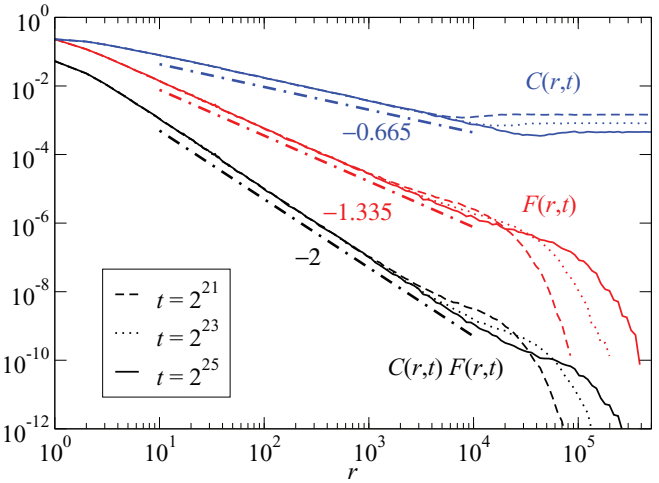

FIG. 5. (Color online) Correlation functions $C(r,t)$ (top three curves) and $F(r,t)$ (middle three curves), and their product (bottom three curves). The dot-dashed lines with indicated slopes are guides to the eyes. The data are obtained for the NCIM with the parameter values $u = 1-v = 0.3$ and $\bar{u} = \bar{v} = 0$. The lattice size is $L = 2^{20}$ and the simulation time is up to $t = 2^{25}$. The data are averaged over more than 100 samples and log-binned.

Accepting the relation (15), we estimate the critical exponent $\alpha = z\delta$ of the NCIM using the indices S_c measured in the previous section. First we need to define the random variable ρ_n. We set $\rho_n = 1$ if site n is occupied by a particle irrespective of its species, and 0 if site n is empty. With this definition, $P_1(b,t) = 1 - P_O(b,t)$ becomes

$$P_1(b,t) = P_A(b,t) + P_B(b,t) + P_X(b,t) + P_Y(b,t). \tag{44}$$

It is convenient to rewrite $P_1(b,t)$ in terms of two-block correlation functions. A block of $\rho_n = A$ may be followed by a block of $\rho_{n+1} = O$, B, or Y. It yields $P_A(b,t) = P_{AO}(b,t) + P_{AB}(b,t) + P_{AY}(b,t)$. One can find the corresponding relations for the others. Thus, we have

$$\begin{aligned} P_1(b,t) = {} & P_{AO}(b,t) + P_{AB}(b,t) + P_{AY}(b,t) \\ & + P_{BO}(b,t) + P_{BA}(b,t) + P_{BX}(b,t) \\ & + P_{XO}(b,t) + P_{XA}(b,t) + P_{XX}(b,t) \\ & + P_{YO}(b,t) + P_{YB}(b,t) + P_{YY}(b,t). \end{aligned}$$

Dividing this with $P_1(2b,t) = 1 - P_{OO}(b)$ and taking the limits, we obtain

$$\begin{aligned} 2^{-\alpha} = {} & S_{AO} + S_{AB} + S_{AY} + S_{BO} + S_{BA} + S_{BX} \\ & + S_{XO} + S_{XA} + S_{XX} + S_{YO} + S_{YB} + S_{YY}. \end{aligned} \tag{45}$$

We evaluate the critical exponent $\alpha = z\delta$ by inserting the numerical values of S_c's into Eq. (45). For example, we obtain that $\alpha \simeq 0.665$ at $u = 0.3$. This value is in perfect agreement with the power-law decay of the correlation function $C(r,t) \sim r^{-\alpha}$ in Fig. 5. It is also consistent with the power-law scaling of

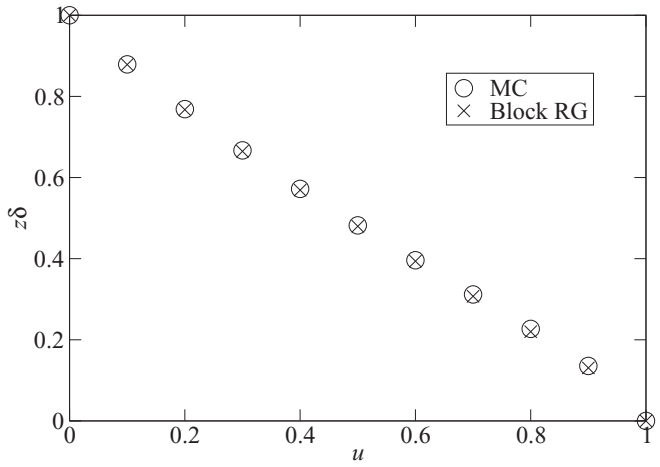

FIG. 6. Comparison of the scaling exponent $z\delta$ obtained from the Monte Carlo simulation of Ref. [5] and the block renormalization analysis.

$F(r,t) \sim r^{-\theta}$ with $\theta = 2 - \alpha$. In Fig. 6, the numerical results for α, thus obtained, are compared with the values obtained from Monte Carlo simulations in Ref. [5]. Both data are in excellent agreement with each other.

We also studied the scaling relation by assigning $\rho_n = 1$ if site n is occupied by A and $\rho_n = 0$ if site n is occupied by B or vacant to get the same result as above (details not shown). Therefore, we conclude that that block renormalization analysis supports the claim that the NCIM exhibits continuously varying critical exponents.

V. SUMMARY AND DISCUSSION

In this paper, we revisited the nonequilibrium chiral Ising model in one dimension using the block renormalization method introduced by Basu and Hinrichsen [10], mainly focusing on the maximal chiral model, which was claimed to have continuously varying exponents [5]. First introducing five different block states reflecting the symmetry of the system as well as the property of having absorbing states, we calculated the asymptotic value of block variable correlation functions that are expected to be universal. It turned out that the ratio of block variable correlation functions varies with a model parameter, which, along with the universality hypothesis, supports the continuously varying nature of the MCM.

We also provided a microscopic theory about the scaling relation Eq. (15), which is associated with the ratio of probability that a block with size b is occupied by at least a single particle with the critical exponent $z\delta$. First, we clarified the necessary conditions that a critical system obeys Eq. (15). Then, we found a relation between two-point correlation functions and the probability that exactly r consecutive sites are empty using a cluster mean-field-type approximation, which is numerically found to be valid for the MCM. Finally, we estimated $z\delta$ using Eq. (15) to find that $z\delta$ is continuously varying and is numerically consistent with the previous numerical results, which again strongly supports the idea that the continuously varying exponents are the inherent feature of the MCM.

Although we neglected the symmetry due to chirality and only kept the feature of having absorbing states when we defined ρ_n in Sec. IV, we obtained the consistent scaling relation. In this sense, the symmetry of the system is not crucial in the block renormalization scheme of the Basu-Hinrichsen formalism, unlike the usual renormalization-group theory. The only important feature, at least for models with absorbing states, is whether the block variable can capture the absorbing state properly.

ACKNOWLEDGMENTS

M.K. acknowledges the financial support from the TJ Park Foundation. S.-C.P. acknowledges the support by the Basic Science Research Program through the National Research Foundation of Korea (NRF) funded by the Ministry of Education, Science and Technology (Grant No. 2011-0014680), and the hospitality of Asia Pacific Center for Theoretical Physics (APCTP). This work is also supported by the Basic Science Research Program through NRF Grant No. 2013R1A2A2A05006776.

[1] R. J. Glauber, J. Math. Phys. **4**, 294 (1963).
[2] A. J. Bray, Adv. Phys. **51**, 481 (2001).
[3] T. J. Newman, A. J. Bray, and M. A. Moore, Phys. Rev. B **42**, 4514 (1990).
[4] A. J. Bray and A. D. Rutenberg, Phys. Rev. E **49**, R27 (1994).
[5] M. Kim, S.-C. Park, and J. D. Noh, Phys. Rev. E **87**, 012129 (2013).
[6] K. Mussawisade, J. E. Santos, and G. M. Schütz, J. Phys. A **31**, 4381 (1998).
[7] N. Menyhárd and G. Ódor, Braz. J. Phys. **30**, 113 (2000).
[8] J. W. Lee and V. Privman, J. Phys. A **30**, L317 (1997).
[9] K. Jain, Europhys. Lett. **71**, 8 (2005).
[10] U. Basu and H. Hinrichsen, J. Stat. Mech.: Theor. Exp. (2011) P11023.
[11] H. J. Maris and L. P. Kadanoff, Am. J. Phys. **46**, 652 (1978).
[12] L. P. Kadanoff, *Statistical Physics: Statics, Dynamics and Renormalization* (World Scientific, Singapore, 2000).
[13] A. P. Solon and J. Tailleur, Phys. Rev. Lett. **111**, 078101 (2013).
[14] K. E. Bassler and B. Schmittmann, Phys. Rev. Lett. **73**, 3343 (1994).
[15] S. B. Dutta and S.-C. Park, Phys. Rev. E **83**, 011117 (2011).
[16] D. ben-Avraham, F. Leyvraz, and S. Redner, Phys. Rev. E **50**, 1843 (1994).
[17] H. Takayasu and A. Y. Tretyakov, Phys. Rev. Lett. **68**, 3060 (1992).
[18] J. T. Cox, Ann. Probab. **17**, 1333 (1989).
[19] T. M. Liggett, *Interacting Particle Systems* (Springer-Verlag, New York, 1995).
[20] V. Belitscky, P. Ferrari, M. Menshikov, and S. Popov, Bernoulli **7**, 119 (2001).

[21] I. M. MacPhee, M. V. Menshikov, S. Volkov, and A. R. Wade, Bernoulli **16**, 1312 (2010).
[22] J. Hooyberghs, F. Iglói, and C. Vanderzande, Phys. Rev. Lett. **90**, 100601 (2003).
[23] T. Vojta and M. Y. Lee, Phys. Rev. Lett. **96**, 035701 (2006).
[24] N. Menyhárd and G. Ódor, Phys. Rev. E **76**, 021103 (2007).
[25] B. Derrida and R. Zeitak, Phys. Rev. E **54**, 2513 (1996).
[26] P.-A. Bares and M. Mobilia, Phys. Rev. Lett. **83**, 5214 (1999).
[27] S.-C. Park, J.-M. Park, and D. Kim, Phys. Rev. E **63**, 057102 (2001).
[28] T. O. Masser and D. ben-Avraham, Phys. Rev. E **64**, 062101 (2001).
[29] D. Toussaint and F. Wilczek, J. Chem. Phys. **78**, 2642 (1983).
[30] K. Kang and S. Redner, Phys. Rev. Lett. **52**, 955 (1984).
[31] M. Bramson and J. L. Lebowitz, Phys. Rev. Lett. **61**, 2397 (1988).
[32] F. Leyvraz and S. Redner, Phys. Rev. A **46**, 3132 (1992).
[33] P. Alemany and D. ben Avraham, Phys. Lett. A **206**, 18 (1995).
[34] P. L. Krapivsky and E. Ben-Naim, Phys. Rev. E **56**, 3788 (1997).
[35] We have performed Monte Carlo simulations to measure $F(r)$ and $C(r)$ at the critical point of the contact process to find an excellent agreement with the scaling relation in (43).